Designing gastric stable adsorption layers by whey protein-pectin complexation at the oil-water interface

Hao Li,* Paul Van der Meeren

Particle and Interfacial Technology Group (PaInT), Department of Green Chemistry and Technology, Faculty of Bioscience Engineering, Ghent University, Coupure Links 653, 9000, Gent, Belgium.

*Corresponding author

Email: Hao.Li@UGent.be

Tel:+32493739118

Abstract

This work aims to design gastric-stable emulsions with food-grade biopolymers, using a novel multi-scale approach. The adsorption layer formation at the oil-water interface was based on opposite charge interactions between whey proteins and pectin (with different esterification levels) at pH 3.0 by a sequential adsorption method. The interfacial assembly and disassembly (interfacial complexation, proteolysis, and lipolysis) during in vitro gastric digestion were evaluated by quartz crystal microbalance with dissipation monitoring, zeta potential, dynamic surface tension, and interfacial dilatational rheology. Besides, the evolution of the particle size and microstructure of bulk emulsions during the digestion was investigated by static light scattering and light microscopy. As compared with WPI-stabilized emulsions, the presence of an additional pectin layer can prevent or at least largely delay gastric destabilization (giving rise to coalescence or/and oiling off). Especially, the esterification degree of the pectin used was found to largely affect the emulsion stability upon gastric digestion.

Keywords:

Gastric digestion, pepsin, gastric lipase, emulsion, interfacial rheology

1. Introduction

Oil-in-water (O/W) emulsions are overwhelmingly present in foods, pharmaceuticals, and personal care products, where they are frequently used as delivery systems for lipophilic ingredients.[1,2] As an ideal delivery system, it is required that the encapsulated functional ingredients can be released from the lipid droplets on demand during the life cycle of the emulsions (e.g. from food processing to after ingestion).

In emulsion systems, oil and water phases are separated by a narrow region, the oil-water interface, which is dominated by emulsifiers to ensure the metastability of the system. Despite the fact that this interface is very thin (in the nanometer range), it represents a large surface area and controls to a great extent the physicochemical stability of emulsions.[3] Thus, interfacial design is a promising way to tailor the functional properties of emulsion systems. The purpose of this study was to design gastric stable adsorption layers using food biopolymers that would enable lipid droplets to survive in harsh gastric digestion conditions (e.g. acid pH, pepsin, gastric lipase), and ultimately be released in the small intestine.

Food proteins exhibit an excellent surface activity in the stabilization of the oil-water interface, whereby submicron or even nano- emulsions can be easily produced. However, the protein layer at the O/W interface is usually vulnerable to pepsin proteolysis. For instance, β-lactoglobulin, a primary protein fraction in milk whey, is resistant to pepsin in bulk solution but can be easily broken down by pepsin once adsorbed onto the oil-water interface due to protein unfolding.[4]

Besides, lipolysis by gastric lipase produces free fatty acids, which are highly surface active and may displace proteins from the O/W interface.[5] The role of gastric lipase has long been neglected for in vitro digestion experiments since human gastric lipase is not commercially available. Sassene et al compared different gastric lipase alternatives for in vitro models of gastric digestion.[6] More recent studies (including the INFOGEST protocol) have suggested that rabbit gastric lipase could be a suitable alternative.[7,8] In fact, in vivo studies have suggested that there is a significant amount of lipolysis that may occur in the stomach, which can account for 10% to 30% of the total amount of lipids that are cleaved in the digestive tract.[9,10] The rupture of the interfacial membrane and lipolysis will affect the stability of emulsions (leading to flocculation/coalescence) and may impact the stability and release of encapsulated bioactive ingredients[11,12] In some cases, insoluble fatty acids produced by gastric lipolysis could also build up at the interface of the emulsion droplets.[13] Furthermore, the work of Golding et al demonstrated that the nature of the interfacial membrane dictates if

the emulsion undergoes simple aggregation or gastric coalescence in both in vitro and in vivo studies.[14,15]

The combination of polysaccharides with proteins could be an effective strategy to modify and extend the functional performance of proteins.[16] Here, it is hypothesized that the indigestibility of polysaccharides could protect the protein-coated droplets during gastric digestion so that a gastric stable emulsion can be made. Since most polysaccharides are not effectively surface active, we used a layer-by-layer technique to allow the adsorption of anionic pectin onto a previously formed protein layer.

The formation of bilayer or multilayer onto emulsion droplets using proteins and polysaccharides has been extensively reported to improve the colloidal stability of the droplets against pH (e.g. around isoelectric point) and ionic strength variations and to retard lipid oxidation during storage.[17,18] However, concerning their gastric stability, the role of an additional polysaccharide layer is still not fully elucidated. Despite the fact that some relevant studies already existed,[19–21] most of them evaluated the gastric stability of multiplayer emulsions using only particle size analysis (e.g. light scattering, microscopy). Emulsion digestion is actually a complicated interface phenomenon.[22] The obtained information from these previous studies may be speculative since it cannot be excluded that the claimed stability or functionalities originate from the bulk coacervation or/and depletion. No more detailed information (e.g. proteolysis kinetics, leakage of the oil core) can be acquired. More importantly, the role of gastric lipase was not taken into account in their in vitro digestion protocols, although gastric lipase has been demonstrated to exhibit a synergistic effect with pepsin on the gastric stability of protein emulsion.[14] Accordingly, the formulation design (especially the choice of polysaccharide) for gastric-stable emulsions remains empirical.

This work aims to elucidate the influence of pectin adsorption on the gastric stability of WPI-coated droplets. Simulated gastric fluids were prepared according to the well-recognized INFOGEST protocol. The digestive enzymes were derived from rabbit gastric extracts so that the combined effect of pepsin and gastric lipase could be evaluated. Since the degree of esterification in pectins can largely influence their physiochemical properties (e.g. electrical properties, gelation properties), both high- and low-methoxy pectin were investigated.

A novel multiscale approach was used to provide insights into the gastric digestion of protein/polysaccharide emulsions. Firstly, the in-situ interfacial assembly of WPI and pectin was investigated by quartz crystal microbalance with dissipation monitoring and zeta-potential analysis. Secondly, the real-time proteolysis and lipolysis at the O/W interface were studied on a single droplet via a modified drop shape tensiometer equipped with a subphase exchange setup. This technique has been demonstrated to study the digestion of a single protein layer

at the oil-water interface,[22] and it is extended to study the properties of the bilayer structures. Besides, the drop tensiometer is able to determine the lipolysis kinetics of triglycerides.[5,23] Finally, the evolution of the particle size, zeta potential, and microstructure of a bulk emulsion during gastric digestion was monitored and quantified.

2. Materials and methods

Whey protein isolate was obtained from Davisco Foods International, Inc. (BiPro, Le Sueur, MN, USA). According to the manufacturer, it contains 92.6% of protein, of which around 85% of the total protein consists of β-lactoglobulin. LMP with a degree of esterification (DE) between 33 and 38% (average molecular weight 45.6 kDa) and HMP with a DE of 68% (average molecular weight 55.8 kDa) were received from Cargill (Ghent, Belgium). They were used without further purification. Medium-chain triglycerides (MCT) were obtained from Go-Keto, containing 60% of C8 and 40% of C10. Florisil® (60–100 mesh for chromatography) was purchased from VWR (Ghent, Belgium). Rabbit gastric extracts (RGE15) were purchased from Lipolytech (Marseille, France), including around 15 U/mg gastric lipase and 500 U/mg pepsin. Curcumin (95%, B21573) was obtained from Alfa Aesar (Germany). Deionized water was used for all experiments. All other chemicals were of analytical grade.

2.1 Dynamic interfacial tension and dilatational rheology

2.1.1 Stock solution preparation

WPI was dissolved in 20 mM sodium phosphate buffer (pH 7.0; ionic strength= 43 mM) at a concentration of 0.1% (w/w). After stirring for 2 h at room temperature and overnight hydration at 4 °C, the WPI dispersion was passed through a 0.45 μm mixed cellulose ester (MCE) membrane filter to remove any insoluble materials. LMP was dissolved in deionized water at a concentration of 0.1% (w/w) after overnight stirring. 0.02% (w/w) of NaN_3 was added into the biopolymer solutions. They were diluted 10-fold by buffers at the tested pHs before using.

The simulated gastric fluid (SGF) used for subphase exchange was prepared according to the INFOGEST protocol, including 0.257 g/L KCl, 0.063 g/L KH_2PO_4, 1.05 g/L $NaHCO_3$, 1.379 g/L NaCl, 0.012 g/L $MgCl_2$, 0.024 g/L $(NH_4)_2CO_3$, 0.011 g/L $CaCl_2(H_2O)_2$, and 1g/L RGE (i.e. containing 15 U/mL lipase and 500 U/mL pepsin). This amount of enzymes was lower than applied during bulk emulsion digestion, but was more than sufficient for observing digestion on a single droplet; it was chosen to avoid a high solution turbidity.

MCT oil mixed with 5% (w/w) Florisil was mildly stirred overnight at room temperature to remove surface active ingredients, and the supernatant was collected and stored at 4 °C for

147 further use. The density of the MCT oil and various solutions was measured at 37 °C by an
148 Anton Paar DMA 5000 M density meter.

149 **2.1.2 In vitro digestion at the oil-water interface**

150 The dynamic surface tension was measured with a modified drop tensiometer allowing
151 external phase exchange (Teclis, Tracker, France), using a 50 mL thermostatted optical glass
152 cuvette containing one or two magnetic stirrers, in combination with the Windrop software
153 (Teclis, France). The temperature was controlled at 37 °C by a Julabo circulator.

154 A rising MCT oil drop (20 µL) was formed at the tip of a U-shaped needle with a diameter of
155 1.61 mm, which was surrounded by 40 mL of 0.01 wt.% WPI solution (pH 7.0). The surface
156 tension was recorded every 5 s. The WPI was allowed to adsorb from the bulk to the interface
157 for around 15,000s before the area deformation was applied and the continuous phase was
158 changed. A peristaltic pump (Ismatec, Germany) with two Teflon tubes was used to perform
159 the exchange of the continuous phase in the cuvette at a flow rate of 11 mL/min. Hereby, the
160 continuous phase was replaced by a 5-fold volume of protein-free pH 7.0 buffer (i.e. about 200
161 mL) and subsequently by a 5-fold volume of fresh pH 3.0 phosphate buffer (20 mM) .

162 To prepare a WPI-pectin bilayer film, the continuous phase was further exchanged with 150
163 mL of 0.01 wt.% LMP or HMP solution in pH 3.0 buffer, followed by 1 hour of equilibration to
164 allow pectin adsorption.

165 Similar protocols were also used to prepare the adsorption layers at pH 5.0.

166 To investigate the role of SGF on the properties of the pre-formed WPI layer or bilayer, the
167 continuous phase was exchanged with 200 mL of SGF (without RGE), followed by 0.5 hour of
168 equilibration. Finally, 40 mL of 1 mg/mL RGE in SGF was introduced to study gastric digestion
169 at the oil-water interface.

170 The dilatational moduli of the interfacial film at the end of each stage were determined at 0.05
171 Hz (i.e. by increasing or decreasing the volume of the oil drop sinusoidally) at an area
172 amplitude of 5%.

173 **2.2 QCM-D and zeta-potential**

174 The sequential adsorption of WPI and pectin at a hydrophobic surface was investigated at pH
175 3.0 by a Q-sense E4 system (Biolin Scientific, Sweden).The QCM-D protocol was according
176 to Li and Van der Meeren (2022).[24] In brief, prior to the measurements, the tubing and chamber
177 were cleaned with a 2% Hellmanex II solution for 40 min at a flow rate of 0.5 mL/min and
178 afterwards rinsed with deionized water overnight at a flow rate of 0.1 mL/min. The temperature
179 during running samples was set at 25.0 °C. Gold-coated crystal sensors (4.95 MHz, QSX 301)

were modified with 2 mM 1-hexadecanethiol in absolute ethanol for at least 20 h to hydrophobize the surface at 30 °C. The hydrated mass of the adsorbed layer was estimated by fitting the frequency and dissipation shifts (based on the 3rd to 11th overtones) with the viscoelastic Kevin-Voigt model using QTools software 30.15.553 (Biolin Scientific). The dynamic viscosity and density of the continuous phase are input parameters for the fitting and were determined to be 0.915 mPa.s and 999.5 at 25.0 °C, respectively.

The zeta-potential of WPI (1 wt.%) and LMP or HMP (0.1 wt.%) as a function of pH was measured with a Zetasizer 3000 (Malvern Panalytical Ltd, Malvern, U.K.)

2.3 Emulsion preparation and characterization

2.3.1 Emulsion preparation

1 wt.% WPI solution was prepared in 10 mM sodium phosphate at pH 3.0. 5 g of MCT oil was added into 45 g of 1 wt.% WPI solution. Subsequently, the mixture was homogenized at 24,000 RPM for 4 min to prepare the WPI emulsion. To remove the excess of non-adsorbed protein, the emulsion was centrifuged at 70 g for 1 hour. The obtained subnatant was removed by a syringe equipped with a long needle, and then replaced with the same amount of the pH 3.0 buffer. Subsequently, the cream layer was dispersed in the buffer by inverting the centrifuge tubes several times. Since some large droplets emerged after the centrifugation step, the WPI-stabilized emulsion was further homogenized at 24,000 RPM for 4 min.

To prepare WPI/pectin bilayer emulsions, 10 g of the washed WPI emulsion was added dropwise into 15 g of 0.5 wt.% pectin solution (adjusted to pH 3.0) under continuous stirring. The excess pectin was also removed by the centrifugation/redispersion steps: the cream layer was dispersed in 19 g of the pH 3.0 buffer. Hence, the final emulsion contained ca. 5 wt.% of MCT oil.

2.3.2 In vitro gastric digestion of emulsion

The in vitro gastric digestion of emulsions was performed according to the INFOGEST method, which is a standardized digestion protocol with international consensus presented by Brodkorb, et al. (2019). The prepared SGF contained 0.514 g/L KCl, 0.126 g/L KH_2PO_4, 2.10 g/L $NaHCO_3$, 2.758 g/L NaCl, 0.024 g $MgCl_2$, 0.048 g $(NH_4)_2CO_3$, 0.022 g/L $CaCl_2(H_2O)_2$, and 8g/L RGEs (i.e. containing 120 U/mL rabbit gastric lipase and 4000 U/mL rabbit pepsin). The SGF was adjusted to pH 3.0 with 6 M HCl at 37 °C. 3 mL of the emulsions was mixed with 3 mL of the SGF (i.e. both in the presence and absence of RGE) in a 15 mL falcon tube. The mixtures were incubated at 37 °C in a water bath under mild orbital shaking. The particle size, zeta-potential, microstructure and interfacial composition of the emulsion droplets as a function of

time (i.e. after 0 min, 10 min, 30 min, 60 min, and 120 min) during digestion were determined according to the following protocols.

2.3.3 Particle size and zeta-potential of emulsion droplets

The particle size of the emulsion droplets was measured before and after in vitro gastric digestion using static light scattering by a MasterSizer 3000 equipped with a Hydro MV unit (Malvern, U.K.). The obscuration value was fixed between 5 and 10% with a stirring speed of 2600 rpm in mixtures of the pH 3.0 phosphate buffer and the SGF (i.e. mixed in an equal volume). The zeta-potential of the emulsion droplets was determined using a Zetasizer 3000 (Malvern Panalytical Ltd, Malvern, U.K.) after 1,000 times dilution by the buffer-SGF mixtures mentioned above. Each individual measurement was an average of three runs.

2.3.4 Microscopy observation

The microstructure of the emulsions before and after in vitro gastric digestion was observed by a CX40 optical microscope (Olympus GmbH, Hamburg, Germany) equipped with an Axiocam ERc5s camera (ZEISS, Germany). The observation was done at a magnification of 100X (i.e. 10X ocular lens and 10X objective lens). Briefly, one drop of the emulsions was placed on a glass slide and covered with a round cover slide to prevent the flow of droplets during observation.

2.4 Migration of encapsulated curcumin

Curcumin-loaded emulsions were prepared according to the protocol described in section 2.2. Curcumin was dissolved in MCT oil at a concentration of 0.05 wt.% by incubation in a water bath at 50˚C for 10 min and subsequent 1 min of ultrasound treatment at room temperature (ca. 20 ˚C). The standard curve of curcumin was set as absorbance values at 425 nm of curcumin diluted in MCT oil in the concentration range from 0.0000625 to 0.0005 wt.%.

The migration of curcumin from emulsion droplets was determined by using a membrane-free model and MCT oil was used as an acceptor medium.[25,26] 5 mL of MCT oil was gently placed on top of 2 mL digestion samples (i.e. already adjusted to pH 7 with NaOH to deactivate the enzymes) in 15 ml falcon tubes. The lower phase but not the upper phase was mildly stirred for 5 min, followed by centrifugation at 1,000 g for 12 min. Subsequently, the curcumin amount in the upper phase was quantified. The migration rate of curcumin (%) was expressed as the amount of migrated curcumin relative to the total curcumin input during emulsion preparation.

2.5 Data analysis

Data were presented as the mean ± standard deviation of at least three independent experiments. The difference between samples was evaluated using one-way ANOVA using GraphPad Prism 9.3 software (San Diego, USA). In some figures regarding interfacial dilatational moduli, the error bars are too small to be visible.

3. Results and discussion

3.1 Interfacial assembly of WPI and LMP/HMP

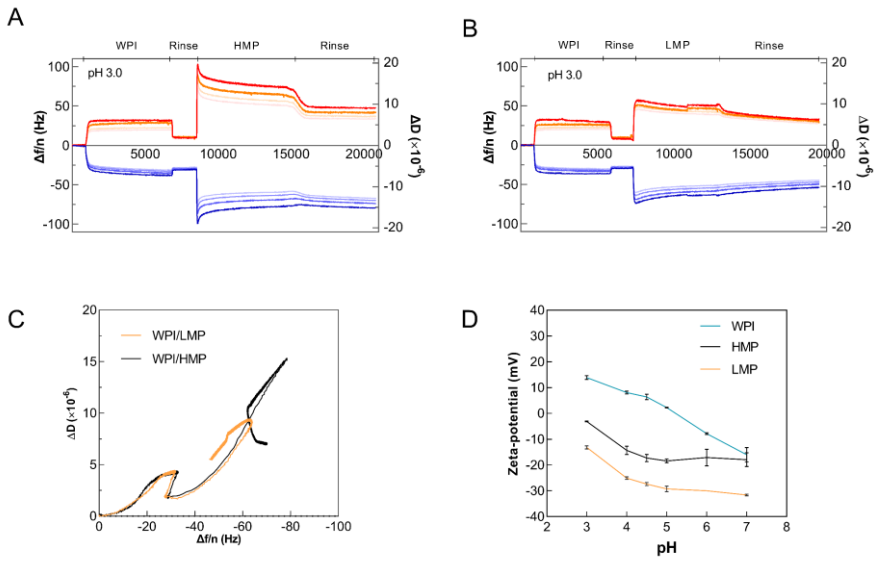

Fig.1 Normalised frequency (blue) and dissipation shifts (red) of the 3rd, 5th, 7th, and 9th overtones (with fading colors for increasing overtones) as a function of time during the sequential adsorption of WPI and HMP (A) or LMP (B) at pH 3.0; ΔD/Δf/n plot at the 7th overtone (C); Zeta-potential as a function of pH (D).

The interfacial assembly of WPI and pectin was tested at pH 3.0 by QCM-D. The alkyl-terminated hydrophobic surface exhibited a water contact angle of 105±2° and was used to mimic the oil-water interface. Initially, the WPI solution was introduced to allow adsorption. After removing excess or loosely bound proteins by a rinsing step, the pectin solution was fed to interact with the pre-formed protein layer and afterwards a rinsing step was carried out.

Figs. 1A and B depicts the frequency (Δf/n) and dissipation shifts (ΔD) as a function of time during the sequential adsorption. WPI led to decreased frequency and increased dissipation. Taking the 5th overtone as an example, the values reached -28±1 Hz and (1.9±0.1)E-6 after rinsing, resp., suggesting a mass uptake (due to WPI adsorption) onto the hydrophobic surface.

By fitting the experimental data with the Voigt model,[27] a wet mass of 6.3±0.8 mg/m^2 was obtained for the WPI layer after a rinsing step at pH 3.0. Note that there should be only a monolayer of whey proteins left on the hydrophobic surface upon the rinsing step (i.e. until a relatively constant frequency and dissipation shifts).[28] Moreover, this value was much higher than the typical surface load (dry mass) of a WPI monolayer (ca. 2 mg/m^2),[29] which implied that the WPI layer at pH 3.0 could entrap about 70 wt.% of water. Comparable hydration degrees were also reported for other globular proteins (e.g. lysozyme and albumin).[30] Upon the introduction of 0.1 wt.% pectin, it can be observed that two types of pectin caused enhanced Δf/n and ΔD shifts both before and after the rinsing step, suggesting the adsorption of pectin onto the protein layer. Besides, the HMP caused more pronounced shifts than the LMP.

Before the rinsing step, the absolute values of these shifts initially increased to a peak value and then decreased gradually, which was thought to be due to slow rearrangements within the interfacial layer and the removal of water molecules. These rearrangements were more obvious in the ΔD-Δf/n plot (which was based on the 7th overtone in **Fig. 1C**), in which the time effect is eliminated. Upon rinsing, the Δf/n and ΔD shifts for WPI-LMP reached -61.5±2.5 Hz and (8.0±0.5)E-6 at the 3rd overtone, -55.1±1.0 Hz and (7.9±1.0)E-6 at the 5th overtone, and -51.0±0.5 Hz and (7.7±0.3)E-6 at the 7th overtone. In contrast, the values for WPI/HMP at the three overtones were -77.5±1.5 Hz and (9.6±0.6)E-6, -71.0±0.5 Hz and (8.1±0.1)E-6, and -67.0±0.2 Hz and (7.0±0.1)E-6, respectively. This also corresponded to a higher hydrated mass for the WPI/HMP bilayer, i.e. about 30 wt.% higher relative to the WPI/LMP case (in **Table 1**). Especially, it was observed that the response of ΔD was more overtone-dependent for WPI/HMP, which indicates more liquid-like characteristics.

This different behaviors can be explained from the zeta-potential as a function of pH, as illustrated in **Fig. 1D**: as compared with HMP, the LMP used had more anionic groups and thus could more strongly (electrostatically) interact with the oppositely charged protein molecules. As a further consequence, the LMP formed a denser composite layer, whereas the adsorbed HMP most probably adopted a more extended conformation (e.g. neutral chains) into the aqueous phase. Besides, the higher adsorbed mass of HMP may be also partly explained by the higher average molecular weight of the HMP compared to the LMP.

Table 1 Hydrated mass of the adsorbed WPI and WPI/pectin layers at pH 3.0.

Samples	Hydrated mass (mg/m^2)
WPI layer	6.3±0.8^c
WPI/LMP bilayer	15.2±1.0^b
WPI/HMP bilayer	20.4±0.6^a

Note: different letters indicate a significant difference.

3.2 In vitro gastric digestion at the O/W interface

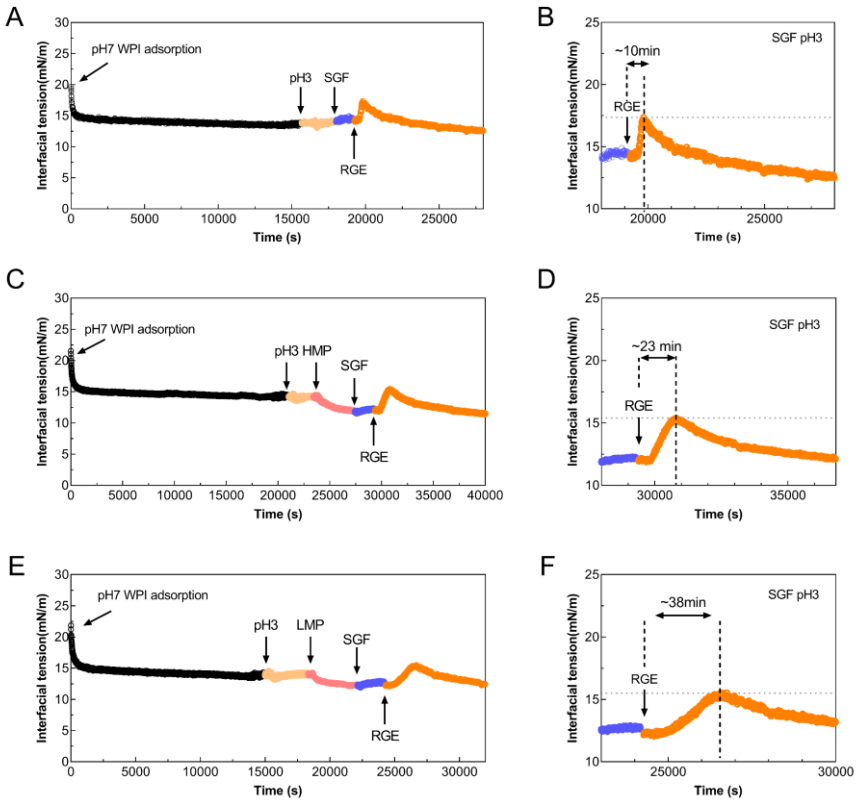

Fig. 2 Interfacial tension as a function of time for the sequential adsorption of 0.01% WPI (at pH 7.0) and 0.01% pectin (at pH 3.0) onto a MCT oil droplet, followed by successive rinsing steps of SGF (with or without RGE), showing the adsorption and digestion of an interfacial WPI layer (A,B), a WPI/HMP bilayer (C,D), and a WPI/LMP bilayer (E,F). Panels B, D, and F

are zoom-in windows of their left counterparts, focusing on the digestion phase. All measurements were performed at 37˚C.

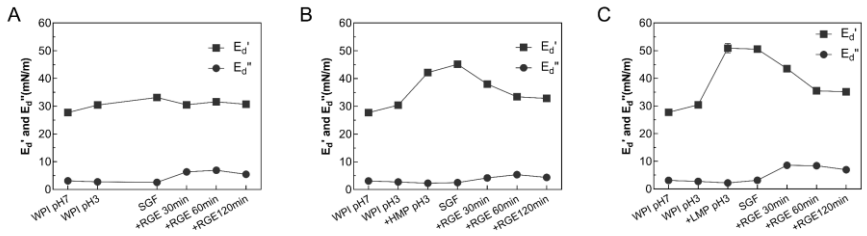

Fig. 3 Interfacial dilatational rheology of the pre-adsorbed WPI layer (at pH 7.0) upon exposure to different environmental conditions, including no pectin (A), HMP (B) or LMP (C), measured at an area amplitude of 5% and a frequency of 0.05 Hz, and represented as the interfacial elastic modulus E_d' (squares) and the interfacial viscous modulus E_d'' (circles). All measurements were performed at 37˚C and pH 3.0.

The evolution of interfacial layer during the simulated gastric digestion was evaluated by interfacial tension and dilatational rheology. In **Fig. 2**, the WPI interfacial layer was prepared after 3 h of adsorption for equilibrium,[24] followed by a rinsing step to remove excess proteins in the bulk. The protein adsorption lowered the interfacial tension of MCT/water from 25.8±0.4 to 13.6±0.5 mN/m. Subsequently, the subphase phase was adjusted to pH 3.0, which did not affect the interfacial tension.

In order to prepare WPI/pectin bilayers, an LMP or HMP solution was introduced to the pre-formed WPI layer at pH 3.0, followed by a rinsing step to remove loosely bound or/and excess pectin. The interfacial tension was only slightly reduced (around 1mN/m) for both LMP and HMP, which is expected since the pectin is less (or not) surface active relative to the proteins. In contrast, the interfacial elastic modulus (E_d') was apparently enhanced, where the E_d' increased from 30.4±0.6 mN/m (for the WPI only) to 42.2±0.2 mN/m for WPI/HMP and to 50.8±1.7 mN/m for WPI/LMP.

As a result of electrostatic attraction, the anionic pectin adsorbs on top of the positively charged protein layer at pH 3.0, thus neutralizing positive charges and facilitating intra-/inter protein interactions, resembling the role of a cross-linker. As discussed above, LMP contained more negative charges, and hence could interact with the protein layer more strongly, forming a more compact composite layer than HMP, in line with the QCM-D results in Section 3.1.

Upon exposure to SGF, the interfacial tension was essentially constant for both WPI and WPI/pectin layers in the absence of rabbit gastric extract (RGE). Additionally, the E_d' was

slightly enhanced (e.g. for the WPI layer and WPI/HMP layer), which may be due to the electrostatic screening effect because of the enhanced ionic strength. This also implied that most pectins remained adsorbed. In contrast, in the presence of RGE (i.e. including pepsin and gastric lipase), for the experiments on WPI, there was a progressive increase in interfacial tension from 13.6±0.5 to 17.5±0.2 mN/m over 10 min. The interfacial tension was then decreased slowly during the rest of the digestion. A similar pattern in interfacial tension was observed for the WPI/HMP and WPI/LMP bilayers, but the first increase was slower and with a smaller magnitude, e.g. from 12.5±0.2 to 15.5±0.2 mN/m in 23 min for WPI/HMP but in 38 min for WPI/LMP. The increase in interfacial tension was mainly ascribed to the proteolysis by pepsin, corresponding to a partial break-up of interfacial protein networks. In the meantime, the gastric lipase may also adsorb onto the O/W interface and lead to lipolysis, as discussed below (digestion at pH 5.0).

As the WPI layer is highly positively charged at pH 3.0, the adsorption of pepsin to the oil-water interface is favored since pepsin exhibits a net negative charge at this pH.[31] With respect to the bilayer structures, it seems that the pepsin still hydrolyzed interfacial proteins, but to a lesser extent since the pepsin adsorption is not favored due to charge inversion upon anionic pectin adsorption. Besides, the steric hindrance effect of the adsorbed pectin chains might play a crucial role as well since a thicker hydrated layer was formed.

Moving now to the interfacial dilatational moduli (**Fig. 3**), for the WPI layer, the E_d' was only slightly decreased after 30 min, but remained basically constant around 30 mN/m during the rest of the digestion phase. For WPI/pectin bilayers, the E_d' gradually decreased over 60 min and then fluctuated between 32 and 35 mN/m, and the E_d'' increased with the digestion, suggesting the break-down of the interfacial protein networks by pepsin. Note that this effect was not due to the desorption of pectins, as discussed below in bulk experiments.

For the individual WPI layer, it is expected that the breakdown of the interfacial film leads to an apparently reduced E_d', whereby the observed phenomena can be due to the adsorption of hydrolyzed peptides and enzymes onto the MCT/water interface.

To further elucidate this process, similar protocols were also performed at pH 5.0. Here, the WPI layer is close to its IEP (i.e. around 5.2 in **Fig. 1**) The pepsin exhibits a much smaller enzyme activity but the activity of gastric lipase becomes much stronger.[32,33] This pH can also simulate the early stage of gastric emptying depending on the meal type.[34–36]

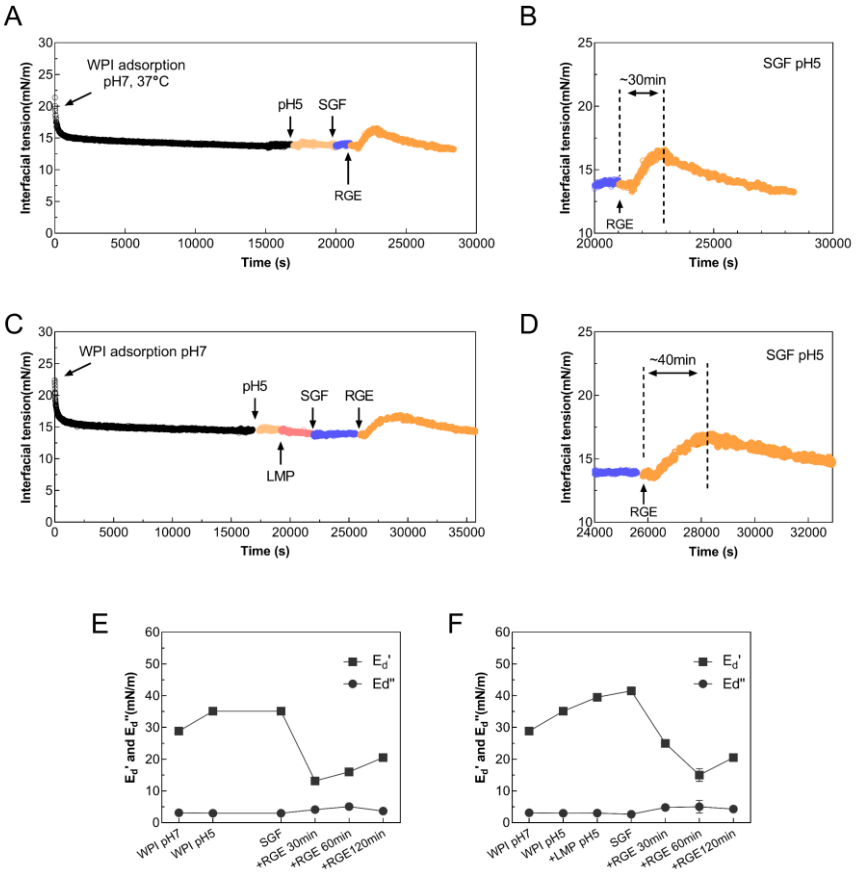

Fig. 4 Interfacial tension as a function of time for pre-adsorbed WPI layer (A) and WPI/LMP bilayer (C) upon exposure to SGF (before or after RGE addition) at pH 5.0 and 37 ˚C; Panels B and D are zoom-in windows of their left counterparts, focusing on the digestion phase; Interfacial dilatational rheology of the pre-adsorbed WPI layer (at pH 7.0) upon exposure to different environmental conditions, including no pectin (E) and in the presence of LMP (F), measured at an area amplitude of 5% and a frequency of 0.05 Hz, and represented as the interfacial elastic modulus E_d' (squares) and the interfacial viscous modulus E_d'' (circles).

In Fig. 4, it can be seen that the pepsin still hydrolyzed the interfacial proteins at pH 5.0 but in a slower way than at pH 3.0. The Interfacial tension gradually went up to 16.4±0.2 mN/m in 30 min and then decreased. Meanwhile, E_d' largely decreased from 35.1±0.7 mN/m to 13.1±1.0 mN/m in 30 min and then increased with time. This confirmed our hypothesis of the initial breakdown of the interfacial network and the subsequent re-formation of the interfacial network by the adsorption of digestive products and enzymes. With respect to the digestion of the WPI-LMP bilayer at pH 5.0, its interfacial tension went up to a maximum value in a slightly slower way than that of the WPI layer, but the magnitude of their maxima was comparable. The E_d' values also supported the delayed interfacial proteolysis in the presence of LMP at pH 5.0. Our previous studies have demonstrated that the LMP adsorption onto the pre-formed layer WPI is more favorable upon lowering the pH from 7.0 to 3.0.[24,28] In pH 3.0-4.0, the WPI and LMP carry opposite charges and the interfacial complexation is most favorable.[24] In pH 5.0-6.5, there is a net electrostatic attraction between the positive patches of whey proteins and anionic LMP, and the LMP adsorption still occurs. However, at pH above 6.5, there is no LMP adsorption on the WPI layer. Additionally, in Fig. 4, the maximum interfacial tension was around 1 mN/m greater than that of the bilayer at pH 3.0 during the digestion. These results pointed to that the protective effect of the additional pectin layer at pH 5.0 on the primary WPI layer was weaker than that at pH 3.0, most probably due to the weaker WPI-pectin interactions and a lower amount of pectin adsorption in the former case.[37]

Therefore, the WPI-pectin bilayer emulsions may only be appropriate for acidic food products with a pH range of 3.0 and 4.0 (i.e. in the presence of strong interfacial complexation) in order to maximize their stabilization performance. In this scenario, consumption of these products (e.g. in a fasted state) does not raise the gastric fluid pH to 5 and higher.

Since the interfacial layer is mainly solid-like, the viscous modulus is not discussed in detail. For all cases, the E_d'' slightly increased with digestion, and then decreased.

In addition to the adsorption of surface-active peptides and enzymes, the gradually reduced surface tension can also be due to the adsorption of free fatty acids (which are more surface active than proteins) at the oil-water interface to some extent.[38] The lipolysis of triglycerides by gastric lipase will indeed produce surface-active free fatty acids, which are expected to displace some proteins from the interface and reduce the interfacial tension and interfacial elasticity. This effect has been proven pronounced for long-chain polyunsaturated fatty acids.[23,39] However, for medium-chain fatty acids, most lipolysis products at the oil-water interface could be released in the aqueous phase instead of being dissolved in the oil core and subsequently adsorbed onto the O/W interface.

In a nutshell, the introduction of pectin (with different degrees of esterification) increased the mechanical strength of the pre-formed protein layer at pH 3.0, which was due to electrostatic attraction-driven interfacial complexation. Furthermore, during simulated gastric digestion, the additional pectin layer apparently delayed the breakdown of the interfacial protein network by pepsin and reduced the extent of proteolysis, possibly due to the combined effect of charge inversion and steric hindrance of pectin chains. The interfacial events relevant to gastric lipase could be overlapped with complex adsorption/desorption phenomena and are complicated to be evaluated by interfacial tension/rheology.

To further evaluate the role of pectin, in vitro gastric digestion was also performed for bulk emulsions.

3.3 In vitro gastric digestion of bulk emulsions

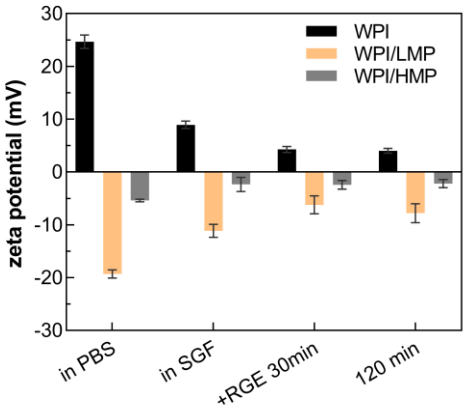

Fig. 5 Evolution of the zeta potential of WPI, WPI/LMP, and WPI/HMP coated droplets before and after in vitro gastric digestion (at pH 3.0). Note: PBS is 10mM phosphate buffer solution at pH 3.0.

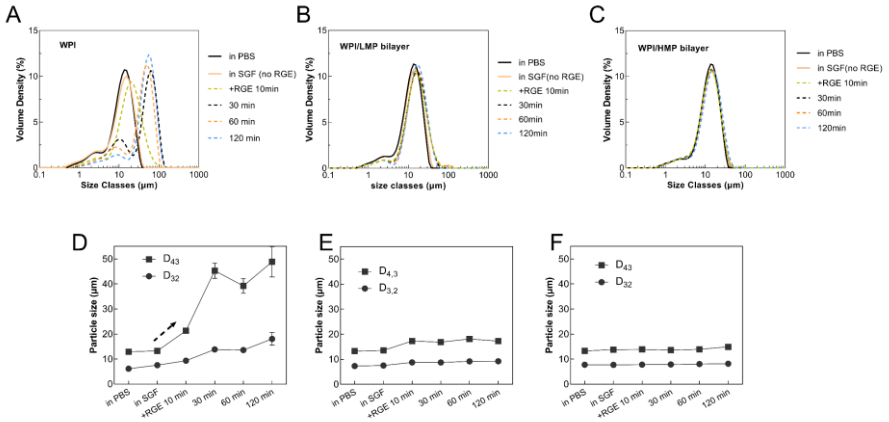

Fig. 6 Evolution of the volume-weighted particle size distribution (A-C) and average size (D_{43} and D_{32}; D-F) of WPI (A,D), WPI/LMP (B,E), and WPI/HMP (C,F) coated droplets before and after in vitro gastric digestion

In **Fig. 5**, the charge inversion of WPI-coated droplets (from positive to negative) upon pectin addition at pH 3.0 clearly suggested forming an additional pectin layer. As expected, the adsorbed LMP layer contained more negative charges than the HMP layer.

The evolution of particle size (distribution) for emulsion droplets stabilized by a WPI layer or a WPI/pectin bilayer was recorded during the simulated gastric digestion (**Fig. 6**). The particle size distribution (PSD) of WPI-coated lipid droplets was characterized by an increasing contribution of larger particles during gastric digestion. In addition to the emulsion droplet flocculation caused by the increased ionic strength in SGF, the increased $D_{4,3}$ and $D_{3,2}$ were primarily due to the proteolysis by pepsin, whereby the broken interfacial film caused droplet coalescence and oiling off. Large oil droplets (i.e. transparent oil phase) were indeed observed after 120 min of gastric digestion, as visualized in the microscopic images in **Fig. 7**.

In contrast, for WPI/LMP-coated droplets, the PSD only slightly shifted to larger size classes. The $D_{4,3}$ and $D_{3,2}$ increased from 13 to 17 μm and from 7.3 to 9.2 μm, respectively, after 10 min of gastric digestion. Subsequently, the particle size essentially kept unchanged. For WPI/HMP bilayer-coated droplets, the particle size distribution remained basically unchanged within the first 60 min. After 120 min of gastric digestion, the $D_{4,3}$ and $D_{3,2}$ increased from 13 and 7.7 μm to 15 and 8.2 μm, resp.

Besides, the microscopic images in **Fig. 7** showed that the WPI/LMP-coated droplets underwent severe droplet flocculation in SGF, whereas this phenomenon was less obvious for

the WPI/HMP-coated droplets. This discrepancy can be due to the fact that the LMP had a higher level of free carboxyl groups, which can be cross-linked by Ca^{2+} or Mg^{2+} (through the "egg-box" model) present in the SGF, thus forming droplet clusters.[40] In this scenario, the lipid droplets can be very weakly bound with each other within these clusters, which can be easily broken down by the continuous stirring applied during particle size analysis by static light scattering. Furthermore, the flocculation became more pronounced in the presence of RGE.

With respect to the zeta-potential (**Fig. 5**), the WPI-coated droplets and bilayer-coated droplets still kept their charge sign but with a smaller absolute value, as compared with the initial droplets. The variation in the ionic strength, binding of counter-ions to the droplet surface, protein displacement by other substances, hydrolysis of protein, and the presence of enzymes (pepsin, gastric lipase) can all be relevant with respect to the reduced magnitude of the zeta-potential.

Overall, there is only limited droplet coalescence occurring in the bilayer emulsion systems (either LMP or HMP) after 120 min of digestion.

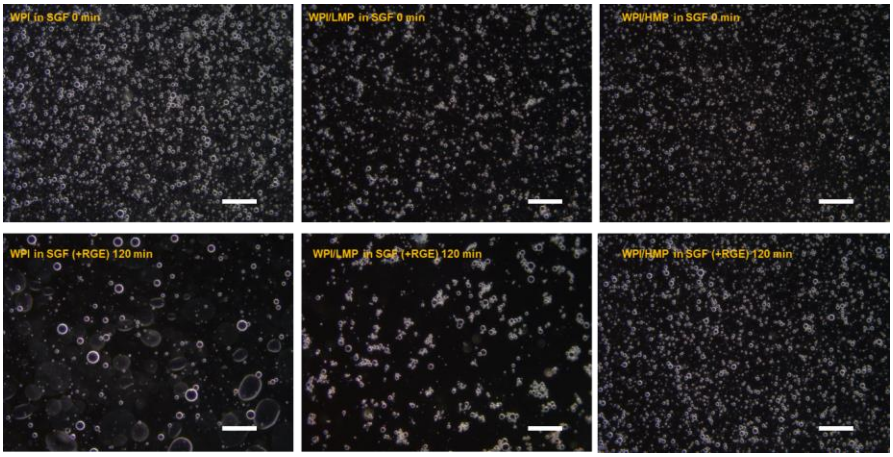

Fig. 7 Microscopic images of WPI-, WPI/LMP-, and WPI/HMP-coated emulsion droplets before (0 min) and after in vitro gastric digestion (120 min). Note: no enzymes were added at 0 min. Scale bar: 20 μm

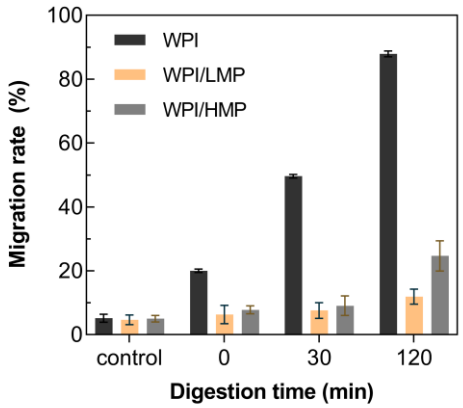

Fig. 8 Migration rate (%) of curcumin from the oil core to an external MCT oil acceptor medium upon in vitro gastric digestion.

In order to quantitively evaluate the protective effect of adsorbed LMP or HMP on the encapsulated oil core, a certain amount of fresh MCT oil was used as an acceptor medium to quantify the migration rate of encapsulated curcumin from the oil core, which can be a facile way to evaluate the quality of emulsions during the digestion process.

In the control group, no RGE and physical centrifugation were present, and the encapsulation efficiency of curcumin was around 95%. At the start of the digestion (0 min), the centrifugation caused the migration of more than 20% of the entrapped curcumin for WPI-coated droplets. After adding RGE, significantly more curcumin migrated during the digestion, reaching 50% after 30 min and over 80% after 120 min.

In contrast, the bilayer emulsions were basically unaffected by the centrifugation step, which can be ascribed to the better mechanical strength of their interfacial layer. During the initial 30 min of digestion, no obvious curcumin migration was observed for either WPI/LMP or WPI/HMP. However, at the end of 120 min digestion, around 25 % of curcumin migrated for WPI/HMP emulsions, whereas this value was only about 12% for WPI/LMP emulsions.

These results suggest that the additional pectin layer can greatly retard the destabilization of protein-coated droplets during gastric digestion. The better performance of WPI/LMP than WPI/HMP can be ascribed to the more rigid interfacial layer, as was also seen from the lower dissipation in QCM-D measurements, as well as the higher interfacial elasticity as observed in interfacial dilatational rheology. Besides, it was reported that pepsin exhibits a net negative charge in the pH range 1.08 to 4.57.[31] The WPI/LMP bilayer has more negative surface

charges, which should electrostatically repel pepsin. These more rigid characteristics may be due to the stronger electrostatic interaction between WPI and LMP (as compared to HMP), as well as to the divalent cations (Ca^{2+} or/and Mg^{2+}) induced cross-linking of LMP chains in SGF.

The different emulsion qualities may impact gastric emptying as well as the release of lipophilic ingredients.[12] Besides, it should be noted that in vivo studies have shown that the coarse, gastric-unstable emulsions could undergo re-emulsification during antral-pyloric transit.[12]

In summary, we investigated the influence of pectin adsorption on the gastric stability of WPI-coated droplets. Both LMP and HMP were able to adsorb onto the WPI layer at pH 3.0 through electrostatic interactions, leading to charge inversion and increased viscoelasticity of the interfacial layer. For the obtained bilayer structures, WPI/HMP adopted a more extended conformation into the aqueous phase, whereas the WPI/LMP formed a compact composite layer. This was primarily due to the different degrees of esterification of the pectins, corresponding to varying charge densities. Interfacial proteolysis led to the break-down of the interfacial protein network, as evidenced by the increased interfacial tension and decreased interfacial dilatational elasticity. In the presence of pectin, the proteolysis was largely delayed (especially for LMP) and its magnitude was reduced. In a later phase, the adsorption of digestive products (e.g. peptides, fatty acids) led to a decreased interfacial tension.

During the gastric digestion of emulsions, extensive coalescence and oiling-off occurred for the WPI-stabilised emulsion. For the WPI/pectin bilayer emulsions (containing either LMP or HMP), no apparent coalescence was observed. However, severe droplet flocculation was observed for the WPI/LMP emulsion, which was thought to be due to the presence of divalent cations in SGF. The WPI/HMP emulsion was essentially stable to flocculation during simulated gastric digestion.

This work may provide useful insights into the formulation design of gastric-stable emulsions with food-grade biopolymers. As our recent studies have demonstrated that the adsorbed pectin exhibits pH-responsive desorption at pH 7, it follows that WPI/pectin bilayer emulsions/microcapsules may be ideal delivery systems to the small intestine.[24] Last but not least, since both protein-polysaccharide electrostatic interactions and gastric enzyme activity are highly pH-dependent, it is of great interest in future studies to employ dynamic in vitro digestion models or in vivo studies to further investigate this type of system.

Acknowledgment

The Chinese Scholarship Council (CSC) is gratefully acknowledged for providing Hao with a PhD scholarship.

References

(1) McClements, D. J.; Decker, E. A.; Weiss, J. Emulsion-Based Delivery Systems for Lipophilic Bioactive Components. *J. Food Sci.* **2007**, *72* (8), R109–R124. https://doi.org/10.1111/j.1750-3841.2007.00507.x.

(2) Luo, Y.; Wang, Q.; Zhang, Y. Biopolymer-Based Nanotechnology Approaches to Deliver Bioactive Compounds for Food Applications: A Perspective on the Past, Present, and Future. *J. Agric. Food Chem.* **2020**, *68* (46), 12993–13000. https://doi.org/10.1021/acs.jafc.0c00277.

(3) Berton-Carabin, C. C.; Sagis, L.; Schroën, K. Formation, Structure, and Functionality of Interfacial Layers in Food Emulsions. *Annu. Rev. Food Sci. Technol.* **2018**, *9* (January), 551–587. https://doi.org/10.1146/annurev-food-030117-012405.

(4) MacIerzanka, A.; Sancho, A. I.; Mills, E. N. C.; Rigby, N. M.; MacKie, A. R. Emulsification Alters Simulated Gastrointestinal Proteolysis of β-Casein and β-Lactoglobulin. *Soft Matter* **2009**, *5* (3), 538–550. https://doi.org/10.1039/b811233a.

(5) Scheuble, N.; Lussi, M.; Geue, T.; Carrière, F.; Fischer, P. Blocking Gastric Lipase Adsorption and Displacement Processes with Viscoelastic Biopolymer Adsorption Layers. *Biomacromolecules* **2016**, *17* (10), 3328–3337. https://doi.org/10.1021/acs.biomac.6b01081.

(6) Sassene, P. J.; Fanø, M.; Mu, H.; Rades, T.; Aquistapace, S.; Schmitt, B.; Cruz-Hernandez, C.; Wooster, T. J.; Müllertz, A. Comparison of Lipases for in Vitro Models of Gastric Digestion: Lipolysis Using Two Infant Formulas as Model Substrates. *Food Funct.* **2016**, *7* (9), 3989–3998. https://doi.org/10.1039/c6fo00158k.

(7) Acquistapace, S.; Patel, L.; Patin, A.; Forbes-Blom, E.; Cuenoud, B.; Wooster, T. J. Effects of Interesterified Lipid Design on the Short/Medium Chain Fatty Acid Hydrolysis Rate and Extent (in Vitro). *Food Funct.* **2019**, *10* (7), 4166–4176. https://doi.org/10.1039/c9fo00671k.

(8) Brodkorb, A.; Egger, L.; Alminger, M.; Alvito, P.; Assunção, R.; Ballance, S.; Bohn, T.; Bourlieu-Lacanal, C.; Boutrou, R.; Carrière, F.; Clemente, A.; Corredig, M.; Dupont,

549 D.; Dufour, C.; Edwards, C.; Golding, M.; Karakaya, S.; Kirkhus, B.; Le Feunteun, S.;
550 Lesmes, U.; Macierzanka, A.; Mackie, A. R.; Martins, C.; Marze, S.; McClements, D.
551 J.; Ménard, O.; Minekus, M.; Portmann, R.; Santos, C. N.; Souchon, I.; Singh, R. P.;
552 Vegarud, G. E.; Wickham, M. S. J.; Weitschies, W.; Recio, I. INFOGEST Static in
553 Vitro Simulation of Gastrointestinal Food Digestion. *Nat. Protoc.* **2019**, *14* (4), 991–
554 1014. https://doi.org/10.1038/s41596-018-0119-1.

555 (9) Armand, M. Lipases and Lipolysis in the Human Digestive Tract: Where Do We
556 Stand? *Curr. Opin. Clin. Nutr. Metab. Care* **2007**, *10* (2), 156–164.
557 https://doi.org/10.1097/MCO.0b013e3280177687.

558 (10) Wooster, T. J.; Moore, S. C.; Chen, W.; Andrews, H.; Addepalli, R.; Seymour, R. B.;
559 Osborne, S. A. Biological Fate of Food Nanoemulsions and the Nutrients They Carry-
560 Internalisation, Transport and Cytotoxicity of Edible Nanoemulsions in Caco-2
561 Intestinal Cells. *RSC Adv.* **2017**, *7* (64), 40053–40066.
562 https://doi.org/10.1039/c7ra07804h.

563 (11) Nguyen, H. T.; Marquis, M.; Anton, M.; Marze, S. Studying the Real-Time Interplay
564 between Triglyceride Digestion and Lipophilic Micronutrient Bioaccessibility Using
565 Droplet Microfluidics. 1 Lab on a Chip Method. *Food Chem.* **2019**, *275*, 523–529.
566 https://doi.org/10.1016/j.foodchem.2018.09.096.

567 (12) Steingoetter, A.; Radovic, T.; Buetikofer, S.; Curcic, J.; Menne, D.; Fried, M.;
568 Schwizer, W.; Wooster, T. J. Imaging Gastric Structuring of Lipid Emulsions and Its
569 Effect on Gastrointestinal Function: A Randomized Trial in Healthy Subjects. *Am. J.*
570 *Clin. Nutr.* **2015**, *101* (4), 714–724. https://doi.org/10.3945/ajcn.114.100263.

571 (13) Pafumi, Y.; Lairon, D.; De La Porte, P. L.; Juhel, C.; Storch, J.; Hamosh, M.; Armand,
572 M. Mechanisms of Inhibition of Triacylglycerol Hydrolysis by Human Gastric Lipase. *J.*
573 *Biol. Chem.* **2002**, *277* (31). https://doi.org/10.1074/jbc.M202839200.

574 (14) Golding, M.; Wooster, T. J.; Day, L.; Xu, M.; Lundin, L.; Keogh, J.; Cliftonx, P. Impact
575 of Gastric Structuring on the Lipolysis of Emulsified Lipids. *Soft Matter* **2011**, *7* (7),
576 3513–3523. https://doi.org/10.1039/c0sm01227k.

577 (15) Keogh, J. B.; Wooster, T. J.; Golding, M.; Day, L.; Otto, B.; Clifton, P. M. Slowly and
578 Rapidly Digested Fat Emulsions Are Equally Satiating but Their Triglycerides Are
579 Differentially Absorbed and Metabolized in Humans. *J. Nutr.* **2011**, *141* (5).
580 https://doi.org/10.3945/jn.110.131110.

581 (16) Li, H.; Wang, T.; Hu, Y.; Wu, J.; Van der Meeren, P. Designing Delivery Systems for

582 Functional Ingredients by Protein/Polysaccharide Interactions. *Trends Food Sci.*
583 *Technol.* **2022**, *119*, 272–287. https://doi.org/10.1016/J.TIFS.2021.12.007.

584 (17) Tian, L.; Zhang, S.; Yi, J.; Zhu, Z.; Li, M.; Decker, E. A.; McClements, D. J. Formation
585 of Antioxidant Multilayered Coatings for the Prevention of Lipid and Protein Oxidation
586 in Oil-in-Water Emulsions: Lycium Barbarum Polysaccharides and Whey Proteins. *J.*
587 *Agric. Food Chem.* **2021**, *69* (51), 15691–15698.
588 https://doi.org/10.1021/acs.jafc.1c06585.

589 (18) Guzey, D.; McClements, D. J. Formation, Stability and Properties of Multilayer
590 Emulsions for Application in the Food Industry. *Adv. Colloid Interface Sci.* **2006**, *128–*
591 *130*, 227–248. https://doi.org/10.1016/j.cis.2006.11.021.

592 (19) Araiza-Calahorra, A.; Sarkar, A. Designing Biopolymer-Coated Pickering Emulsions to
593 Modulate: In Vitro Gastric Digestion: A Static Model Study. *Food Funct.* **2019**, *10* (9),
594 5498–5509. https://doi.org/10.1039/c9fo01080g.

595 (20) Xu, D.; Yuan, F.; Gao, Y.; Panya, A.; McClements, D. J.; Decker, E. A. Influence of
596 Whey Protein-Beet Pectin Conjugate on the Properties and Digestibility of β-Carotene
597 Emulsion during in Vitro Digestion. *Food Chem.* **2014**, *156*, 374–379.
598 https://doi.org/10.1016/j.foodchem.2014.02.019.

599 (21) Sabet, S.; Rashidinejad, A.; Qazi, H. J.; McGillivray, D. J. An Efficient Small Intestine-
600 Targeted Curcumin Delivery System Based on the Positive-Negative-Negative
601 Colloidal Interactions. *Food Hydrocoll.* **2021**, *111*, 106375.
602 https://doi.org/10.1016/j.foodhyd.2020.106375.

603 (22) Maldonado-Valderrama, J. Probing in Vitro Digestion at Oil–Water Interfaces. *Curr.*
604 *Opin. Colloid Interface Sci.* **2019**, *39*, 51–60.
605 https://doi.org/10.1016/j.cocis.2019.01.004.

606 (23) Labourdenne, S.; Gaudry-Rolland, N.; Letellier, S.; Lin, M.; Cagna, A.; Esposito, G.;
607 Verger, R.; Rivière, C. The Oil-Drop Tensiometer: Potential Applications for Studying
608 the Kinetics of (Phospho)Lipase Action. *Chem. Phys. Lipids* **1994**, *71* (2), 163–173.
609 https://doi.org/10.1016/0009-3084(94)90068-X.

610 (24) Li, H.; Van der Meeren, P. Sequential Adsorption of Whey Proteins and Low Methoxy
611 Pectin at the Oil-Water Interface: An Interfacial Rheology Study. *Food Hydrocoll.*
612 **2022**, *128*, 107570. https://doi.org/10.1016/J.FOODHYD.2022.107570.

613 (25) Beicht, J.; Zeeb, B.; Gibis, M.; Fischer, L.; Weiss, J. Influence of Layer Thickness and
614 Composition of Cross-Linked Multilayered Oil-in-Water Emulsions on the Release

Behavior of Lutein. *Food Funct.* **2013**, *4* (10), 1457–1467. https://doi.org/10.1039/c3fo60220f.

(26) Wilson, A.; Ekanem, E. E.; Mattia, D.; Edler, K. J.; Scott, J. L. Keratin-Chitosan Microcapsules via Membrane Emulsification and Interfacial Complexation. *ACS Sustain. Chem. Eng.* **2021**, *9* (49), 16617–16626. https://doi.org/10.1021/acssuschemeng.1c05304.

(27) Reviakine, I.; Johannsmann, D.; Richter, R. P. Hearing What You Cannot See and Visualizing What You Hear: Interpreting Quartz Crystal Microbalance Data from Solvated Interfaces. *Anal. Chem.* **2011**, *83* (23), 8838–8848. https://doi.org/10.1021/ac201778h.

(28) Li, H.; Wu, J.; Doost, A. S.; Su, J.; Van der Meeren, P. Electrostatic Interaction between Whey Proteins and Low Methoxy Pectin Studied by Quartz Crystal Microbalance with Dissipation Monitoring. *Food Hydrocoll.* **2021**, *113* (November 2020), 106489. https://doi.org/10.1016/j.foodhyd.2020.106489.

(29) Setiowati, A. D.; Saeedi, S.; Wijaya, W.; Van der Meeren, P. Improved Heat Stability of Whey Protein Isolate Stabilized Emulsions via Dry Heat Treatment of WPI and Low Methoxyl Pectin: Effect of Pectin Concentration, pH, and Ionic Strength. *Food Hydrocoll.* **2017**, *63*, 716–726. https://doi.org/10.1016/j.foodhyd.2016.10.025.

(30) Ouberai, M. M.; Xu, K.; Welland, M. E. Effect of the Interplay between Protein and Surface on the Properties of Adsorbed Protein Layers. *Biomaterials* **2014**, *35* (24), 6157–6163. https://doi.org/10.1016/j.biomaterials.2014.04.012.

(31) Andreeva, N. S.; James, M. N. G. Why Does Pepsin Have a Negative Charge at Very Low pH? An Analysis of Conserved Charged Residues in Aspartic Proteinases. *Adv. Exp. Med. Biol.* **1991**, *306*, 39–45. https://doi.org/10.1007/978-1-4684-6012-4_4.

(32) Salelles, L.; Floury, J.; Le Feunteun, S. Pepsin Activity as a Function of PH and Digestion Time on Caseins and Egg White Proteins under Static: In Vitro Conditions. *Food Funct.* **2021**, *12* (24), 12468–12478. https://doi.org/10.1039/d1fo02453a.

(33) Sams, L.; Paume, J.; Giallo, J.; Carrière, F. Relevant pH and Lipase for in Vitro Models of Gastric Digestion. *Food Funct.* **2016**, *7* (1), 30–45. https://doi.org/10.1039/c5fo00930h.

(34) Dong, L.; Wu, K.; Cui, W.; Fu, D.; Han, J.; Liu, W. Tracking the Digestive Performance of Different Forms of Dairy Products Using a Dynamic Artificial Gastric Digestive System. *Food Struct.* **2021**, *29*. https://doi.org/10.1016/j.foostr.2021.100194.

heeft verwijderd: PH

heeft verwijderd: PH

heeft verwijderd: PH

(35) Amara, S.; Bourlieu, C.; Humbert, L.; Rainteau, D.; Carrière, F. Variations in Gastrointestinal Lipases, pH and Bile Acid Levels with Food Intake, Age and Diseases: Possible Impact on Oral Lipid-Based Drug Delivery Systems. *Adv. Drug Deliv. Rev.* **2019**, *142*, 3–15. https://doi.org/10.1016/j.addr.2019.03.005.

(36) Dekkers, B. L.; Kolodziejczyk, E.; Acquistapace, S.; Engmann, J.; Wooster, T. J. Impact of Gastric pH Profiles on the Proteolytic Digestion of Mixed Blg-Xanthan Biopolymer Gels. *Food Funct.* **2016**, *7* (1), 58–68. https://doi.org/10.1039/c5fo01085c.

(37) Benjamin, O.; Silcock, P.; Leus, M.; Everett, D. W. Multilayer Emulsions as Delivery Systems for Controlled Release of Volatile Compounds Using pH and Salt Triggers. *Food Hydrocoll.* **2012**, *27* (1), 109–118. https://doi.org/10.1016/j.foodhyd.2011.08.008.

(38) Infantes-Garcia, M. R.; Verkempinck, S. H. E.; Del Castillo-Santaella, T.; Maldonado-Valderrama, J.; Hendrickx, M. E.; Grauwet, T. In Vitro Gastric Lipid Digestion of Emulsions with Mixed Emulsifiers: Correlation between Lipolysis Kinetics and Interfacial Characteristics. *Food Hydrocoll.* **2022**, *128*, 107576. https://doi.org/10.1016/j.foodhyd.2022.107576.

(39) Reis, P.; Miller, R.; Leser, M.; Watzke, H.; Fainerman, V. B.; Holmberg, K. Adsorption of Polar Lipids at the Water-Oil Interface. *Langmuir* **2008**, *24* (11), 5781–5786. https://doi.org/10.1021/la704043g.

(40) Cao, L.; Lu, W.; Mata, A.; Nishinari, K.; Fang, Y. Egg-Box Model-Based Gelation of Alginate and Pectin: A Review. *Carbohydr. Polym.* **2020**, *242*, 116389. https://doi.org/10.1016/j.carbpol.2020.116389.

heeft verwijderd: PH

heeft verwijderd: PH

heeft verwijderd: PH

684 ## Table of contents (TOC)

685

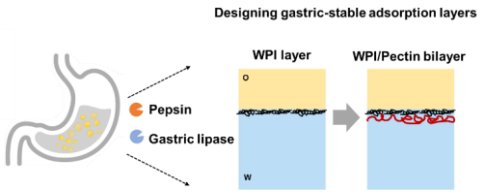

686

687

688